Title: Magnetofluidic platform for rapid multiplexed screening of SARS-CoV-2 variants and respiratory pathogens

Authors: Alexander Y. Trick[1]*, Fan-En Chen[1]*, Liben Chen[2]**, Pei-Wei Lee[2], Alexander C. Hasnain[1], Heba H. Mostafa[3], Karen C. Carroll[3], Tza-Huei Wang[1,2,4]**

*Co-first author

**Co-corresponding author

[1]Department of Biomedical Engineering, Johns Hopkins University, Baltimore, MD 21218, USA

[2]Department of Mechanical Engineering, Johns Hopkins University, Baltimore, MD 21218, USA

[3]Division of Medical Microbiology, Department of Pathology, Johns Hopkins University School of Medicine, Baltimore, MD 21205, USA

[4]Institute for NanoBiotechnology, Johns Hopkins University, Baltimore, MD 21218, USA

Abstract

The rise of highly transmissible SARS-CoV-2 variants brings new challenges and concerns with vaccine efficacy, diagnostic sensitivity, and public health responses in the fight to end the pandemic. Widespread detection of variant strains will be critical to inform policy decisions to mitigate further spread, and post-pandemic multiplexed screening of respiratory viruses will be necessary to properly manage patients presenting with similar respiratory symptoms. In this work, we have developed a portable, magnetofluidic cartridge platform for automated PCR testing in <30 min. Cartridges were designed for multiplexed detection of SARS-CoV-2 with either distinctive variant mutations or with Influenza A and B. The platform demonstrated a limit of detection down to 2 copies/µL SARS-CoV-2 RNA with successful identification of B.1.1.7 and B.1.351 variants. The multiplexed SARS-CoV-2/Flu assay was validated using archived clinical nasopharyngeal swab eluates (n = 116) with an overall sensitivity/specificity of 98.1%/95.2%, 85.7%/100%, 100%/98.2%, respectively, for SARS-CoV-2, Influenza A, and Influenza B. Further testing with saliva (n = 14) demonstrated successful detection of all SARS-CoV-2 positive samples with no false-positives.

Introduction

While the development and distribution of vaccines brings hope for a return to normalcy, extensive diagnostic testing remains critical to curbing the spread of the SARS-CoV-2 virus[1–3]. Even with vaccines, the rise of highly transmissible virus variants that have dominated recent coronavirus disease 2019 (COVID-19) outbreaks raises concerns about mutations leading to potential escape from vaccine protection[4–6]. Insufficient screening and surveillance has left public health officials with large gaps in knowledge of the extent and impact of these variants[7]. Furthermore, demand for testing will continue after the pandemic wanes, as it is predicted that COVID-19 will maintain circulation alongside other seasonal or endemic respiratory viruses presenting with similar symptoms, such as influenza[8]. Multiplexed diagnostic screening for detection of SARS-CoV-2 variants and other respiratory pathogens must be made widely accessible to provide targeted treatments to patients and notify policy makers if more stringent measures are needed to control transmission.

38   Broad identification of virus variants and infectious pathogens can be achieved with genomic
39 sequencing, but the necessary equipment and data processing required to conduct sequencing
40 procedures is currently prohibitively expensive and complex for universal adoption[9]. Instead of
41 sequencing, nucleic acid amplification tests (NAATs) typically used for infectious disease diagnosis may be
42 readily modified to detect characteristic sequences of variants[10]. Although relatively easy to implement
43 compared to sequencing, the increase in demand for NAATs during the SARS-CoV-2 pandemic has
44 revealed severe deficiencies in public access to infectious disease diagnostics and aggravated existing
45 shortages in testing capacity, supplies, and laboratory personnel[11].

46   The gold standard NAATs for detection of SARS-CoV-2 RNA and other respiratory viruses use
47 reverse-transcription polymerase chain reaction (RT-PCR)[12]. These tests provide the greatest sensitivity
48 and specificity, but often require transport to high complexity laboratories in centralized test facilities
49 which can lead to large backlogs with turnaround times of days or weeks[11,13]. Test results should ideally
50 be delivered on-site at the testing location to facilitate recording of accurate surveillance data and to
51 enable immediate notification of the test results to the patient for initiating quarantine or linkage to care.
52 Currently available rapid NAAT platforms use expensive instruments and test cartridges making rapid
53 screening for a large population with these systems unrealistic. Because of the long turnaround times and
54 high cost per test of current NAAT platforms, many strategies for large scale testing opt for cheaper
55 antigen tests[14]. Compared to PCR, these viral antigen tests have reduced sensitivity, higher rates of false-
56 positives, and are not easily amenable to multiplexed detection of several genetic targets or
57 pathogens[15,16].

58   To address the need for affordable and accessible multiplexed NAATs with a fast turnaround time,
59 we developed an imaging-based portable droplet magnetofluidic cartridge platform. Instead of traditional
60 fluidic strategies for sample handling and assay automation, droplet magnetofluidic technologies use the
61 movement of magnetic beads through discrete droplets of reagents to capture, purify, and transfer
62 analytes for amplification and/or detection[17–20]. Recent developments of magnetofluidic cartridges have
63 integrated static assay reagents isolated by immiscible liquid barriers into a low-cost plastic disposable[21–
64 23]. Magnetic transfer of beads along a hydrophobic surface within the cartridges obviates the need for
65 precision fluidic channels and flow controllers that increase the complexity and cost of other automated
66 NAAT platforms[24,25]. While previous studies using magnetofluidic cartridges were limited to a single
67 reaction well per cartridge, this work achieves higher levels of multiplexed detection through a
68 combination of duplexed PCR probe assays and a novel multi-elution aliquoting scheme to distribute
69 nucleic acids.

70   Testing with our platform's disposable cartridges enables sample-to-answer RT-PCR in under 30
71 minutes with detection of up to 4 genetic targets per test. Two different assay cartridges were designed
72 – one for SARS-CoV-2 detection and differentiation of its variants, and another for multiplexed screening
73 of SARS-CoV-2 with Influenza A, and Influenza B. We demonstrated the utility of our cartridge assays by
74 testing with extracted RNA from clinical samples, nasopharyngeal swab eluates, and saliva samples. This
75 platform presents a potent opportunity to expand access to screening SARS-CoV-2 variants and
76 multiplexed respiratory pathogen testing in any setting with minimal training and immediate on-site
77 reporting of results.

78 **Results**

79 ***Assay design and workflow***

80   To conduct a test, the sample is first mixed with a buffer containing functionalized magnetic beads
81   followed by loading the entire mixture into the sample port of the cartridge. Once sealed with an adhesive
82   tab to prevent leakage of the sample, the cartridge is inserted into a slot in the side of the instrument (Fig.
83   1a, Supplementary Fig. 1). Identifying information for the sample is entered by the user using the
84   instrument's touchscreen interface followed by full automation of nucleic acid extraction, purification,
85   and amplification by RT-PCR. The instrument conducts real-time analysis of fluorescent signals with fully
86   interpreted results displayed on the screen in under 30 minutes. Each instrument has a compact footprint
87   (14.5 cm x 21.6 cm x 14.5 cm) and built-in wireless connectivity for potential integration with laboratory
88   information systems.

89   We designed two different cartridge assays (Fig. 1b-c) for either detection of SARS-CoV-2 variants
90   of concern, or multiplexed diagnosis of SARS-CoV-2 with Influenza A and B. Both cartridges employ two
91   duplexed PCR assays in separate wells containing hydrolysis probes labelled with FAM or Cy5/TYE
92   fluorophores for a total of 4 target sequences per cartridge. To ensure cartridge reagents are functional
93   and sample processing is fully completed, each cartridge assay detects a synthetic control RNA sequence[26]
94   that is pre-mixed in the magnetic bead solution. Detection of SARS-CoV-2 and control RNA are duplexed
95   in the first well in both assays. A conserved nucleocapsid gene (N1) target sequence was adopted for
96   universal detection of SARS-CoV-2[27].

97   The cartridge for discrimination of SARS-CoV-2 variants uses the second PCR well for primers and
98   probes designed by Vogel et al.[10] to detect the presence of distinct mutations in the SARS-CoV-2 spike
99   (Δ69-70) and ORF1a (Δ3675-3677) genes (Fig. 1b). The Δ69-70 mutation is associated uniquely with the
100   B.1.1.7. variant that has shown high transmissibility.[4,5] Meanwhile, the ORF1a deletion is found in B.1.1.7,
101   B.1.351, and P.1 variants of concern [10]. Therefore, if both the spike and the ORF1a mutation are present,
102   the virus is classified as B.1.1.7. If the spike mutation is not detected, but the ORF1a mutation is, then the
103   virus is classified as potentially B.1.351 or P.1. The PCR probes produce an amplification signal in virus
104   lineages *not* included within the variants of concern, while signal dropout occurs if the described
105   mutations are present. In the second cartridge designed for multiplexed detection of SARS-CoV-2 with
106   influenza A and B, the second PCR well instead contains a duplex assay containing primers and probes for
107   influenza A and B detection[28–30] (Fig. 1c).
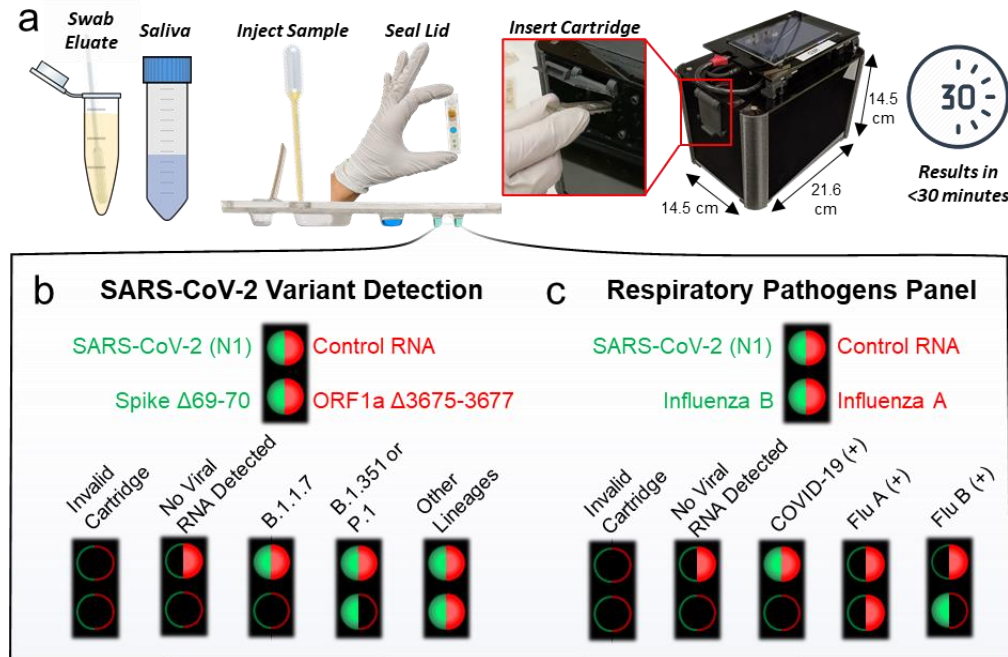
Fig. 1| Cartridge platform operation. a, Nasal swab eluate or saliva is injected directly into the cartridge with magnetic beads followed by sealing the cartridge and inserting it into the instrument. After magnetofluidic sample preparation and PCR, the instrument reports the assay results on the built-in touchscreen within 30 minutes. **b,** Each PCR well contains two fluorescent probes in the FAM (green/left) or Cy5 (red/right) spectrum. Cartridges include a duplexed assay for the conserved N1 SARS-CoV-2 sequence and control RNA in the first well. The cartridge designed for detection of SARS-CoV-2 variants includes a duplexed PCR assay in the second well with probes spanning regions that contain deletions found in variants of concern. A lack of amplification in the second well indicates the presence of a mutation and can be used to classify the type of variant present. **c,** Cartridges designed for multiplexed detection of respiratory pathogens have a duplexed Influenza A and Influenza B PCR assay in the second well.
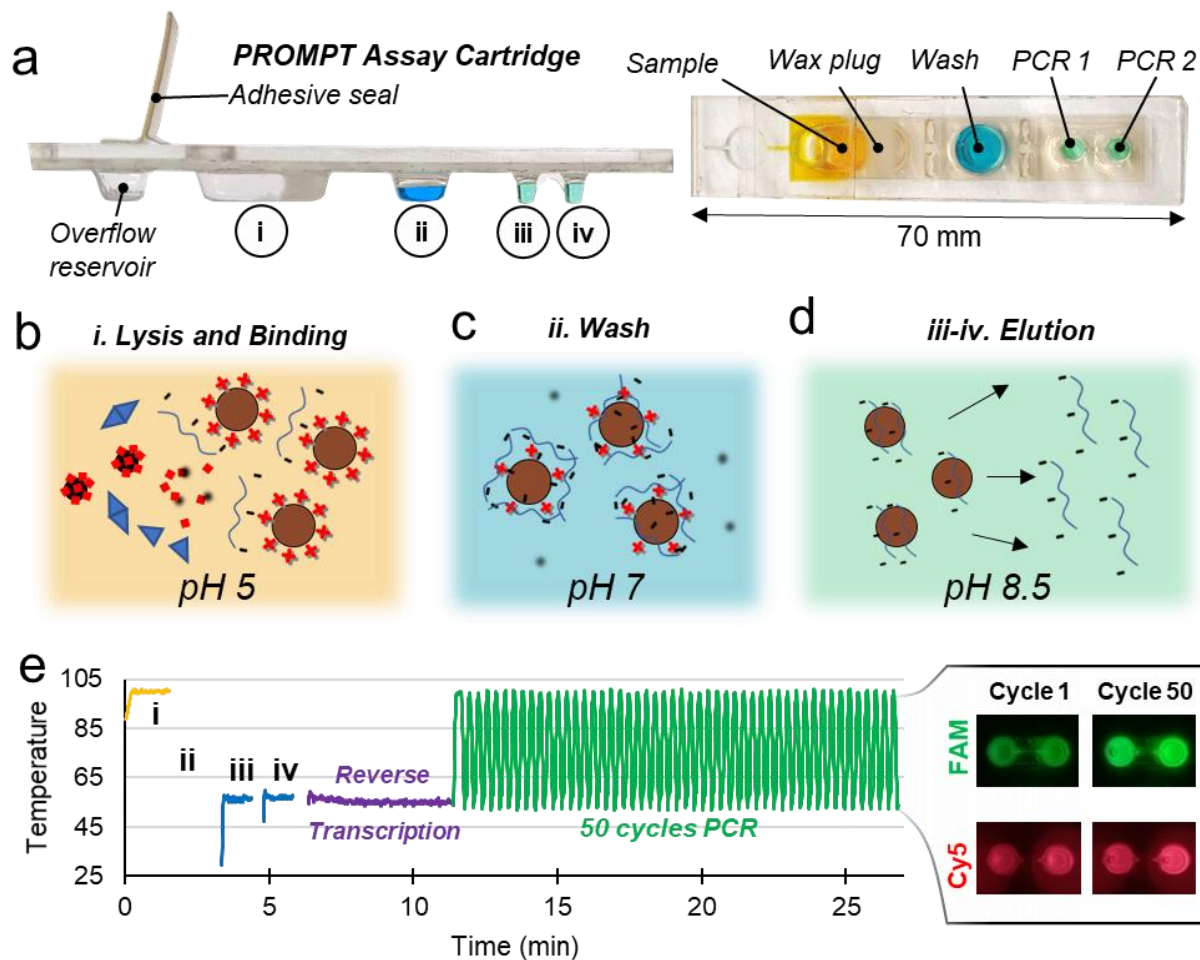
Magnetofluidic cartridge design

The thermoplastic cartridge design in this work builds upon previous developments of magnetofluidic cartridges by incorporating greater flexibility in sample input volume, higher multiplexing of biomarkers, and more robust construction for easier handling[21–23]. Construction of the cartridges uses simple lamination techniques of three layers that have been laser-cut and thermoformed (Supplementary Fig. 2). All reagents are pre-loaded into extruded thermoformed wells of the cartridge (Fig. 2a) except for the magnetic beads which are mixed with the sample prior to loading into the cartridge. An immiscible layer of silicone oil provides an evaporation barrier and a fluidic interconnect between reagent wells for transfer of the magnetic beads.   By isolating the reagents in thin-walled thermoformed wells, the thermal mass of the reaction can be spatially isolated for targeted, rapid thermocycling leading to faster turnaround times than traditional bulky PCR systems.

Once the sample is mixed with the magnetic bead buffer and loaded into the cartridge, the viral particles are lysed with surfactant and heating in the first well to allow for electrostatic binding of viral RNA to the charge-functionalized magnetic beads (Fig. 2b). Transfer of the beads into the second well exchanges the beads into a pH neutral wash buffer for removal of binding salts and any contaminants in the sample which may inhibit PCR (Fig. 2c). Finally, sequential transfer of the beads into the alkaline (pH

134 8.5) PCR wells allows for neutralization of the bead coating and partial release of captured RNA into each
135 PCR reaction well (Fig. 2d) for amplification and fluorescence detection. To achieve under 30-minute
136 turnaround time, sample preparation from lysis to completion of elution takes around 6 minutes, followed
137 by 5 minutes of reverse transcription, and 50 cycles of PCR thermocycling in under 18 minutes (Fig. 2e).

138 The cartridge in this work includes several key innovations. A wax plug between the sample well
139 and wash well seals off the oil and downstream reagents to immobilize all downstream fluids during
140 transport and handling, which allows for full range of tilting and shaking the cartridge without reagent
141 leakage. After the user injects the sample into the cartridge port, any excess sample can escape into an
142 overflow reservoir and the port is sealed with an adhesive strip to provide an additional layer of safety
143 from sample contamination and spill of infectious materials.

144 The most critical innovation in this work is the inclusion of an additional PCR well for higher levels
145 of multiplexing coupled with a sequential elution strategy. Sequential elution takes advantage of the
146 incomplete release of captured nucleic acids to aliquot RNA into separate reaction buffers. As the beads
147 are exposed to each new buffer, the captured nucleic acids will be released until an equilibrium between
148 the concentration of analyte on the bead surface and in the reaction buffer is reached. We have
149 demonstrated this technique has potential to expand multiplexing up to at least six separate reactions
150 (Supplementary Fig. 3). This flexibility in multiplexing provides an option to expand future cartridges to
151 include additional targets for other SARS-CoV-2 variants or for a larger panel of pathogens.

Fig. 2| Cartridge design. a, The magnetofluidic cartridge contains preloaded assay reagents for sample purification and PCR. A layer of silicone oil fills the space within the cartridge between reagents, and a wax plug prevents the reagents from leaking during transport such that the first well remains empty for loading the sample. **b,** The first well is heated to 100°C for 80 seconds (i) to promote viral lysis for RNA capture and to release the wax plug at the base of the sample well to allow passage of magnetic beads. **c,** Bead transfer into the wash well (ii) promotes removal of salts, proteins, and other sample components that may inhibit PCR. **d,** Bead transfer into the PCR wells accompanied by heating to 55°C (iii, iv) allows sequential elution of the captured RNA. **e,** Plot of the temperature of previously described steps for sample preparation followed by one-pot reverse transcription and PCR with real-time 2-color fluorescence detection of both reaction wells at each cycle.

Instrument design and sample processing

The instrument contains all components necessary for transfer of magnetic beads through the cartridge, temperature control to melt wax seals and conduct RT-PCR, and optics for fluorescence excitation and detection (Fig. 3a-b). Instead of complex fluidics, valves, and pressure controllers typically found in microfluidic instrumentation, the components here include primarily low-cost hobby servo motors and off-the-shelf LED and CMOS camera parts (Supplementary Table 1). Once the cartridge is inserted into the instrument, it is detected with the CMOS camera, which uses the fluorescent outline of the PCR wells to determine if the cartridge is properly positioned. The fluorescence detection uses dual bandpass filters over the CMOS camera for emission, and over a 2-color LED for excitation to permit multi-

171   color detection without moving parts by alternating blue and red LED illumination for FAM and Cy5/TYE
172   fluorophores, respectively. Three servo motors automate application of the heat blocks to the cartridge
173   and magnetic bead transfer (Supplementary Fig. 4). If the cartridge has been inserted fully, then the first
174   servo motor involved rotates a shaft to mount both the sample heat block and PCR heat block onto the
175   cartridge. With the heat blocks mounted, a power resistor heats the sample heat block to 100°C for 80
176   seconds to both promote viral lysis and melt the wax plug which then floats toward the top of the cartridge
177   leaving a clear passage for transfer of the magnetic particles (Fig. 3c).

178   A second servo motor swivels two opposing neodymium permanent magnets to the bottom or
179   top of the cartridge to pellet beads into reagent wells or extract them into the oil layer. The third servo
180   motor translates this magnet arm along the length of the cartridge for transfer of the beads between wells
181   through the oil (Supplementary Video 1). This magnetic transfer paradigm allows the beads to be
182   transferred anywhere along the long axis of the cartridge for compatibility with cartridge designs
183   constructed with varying well number, dimensions, and positioning. With the wax melted, the beads are
184   collected out of the sample well to the top of the cartridge and transferred into the wash buffer well to
185   remove contaminants that might inhibit function of the downstream PCR assays (Fig. 3d). After alternate
186   application of the top and bottom magnets for three repeated exchanges of the beads into and out of the
187   wash buffer, the beads are finally transferred sequentially into the PCR wells (Fig. 3e). Each well receives
188   the beads for 1 minute while the PCR buffers are heated to 55°C to facilitate release of the capture RNA
189   and initiate reverse transcription. This multi-elution strategy permits some control over the release of
190   RNA with higher elution temperature providing a higher fraction of RNA recovered in each well (Fig. 3f).

191   Immediately after elution, generation of cDNA and amplification is carried out with reverse
192   transcription and PCR thermocycling. Temperature in both wells is simultaneously controlled by the PCR
193   heat block with 2 second holds at 100°C for cDNA denaturation followed by 2 seconds at 55°C for
194   annealing and extension. Miniaturization of the PCR heat block's thermal mass and the use of copper's
195   high thermal conductivity (~400 W/m-K) enables rapid changes in temperature powered by a heatsinked
196   thermoelectric element (Supplementary Fig. 5). The optimized heat block has temperature ramp rates
197   ranging between 6 to 10°C/s for both heating and cooling. When combined with time required for
198   denaturation and annealing holds, controlled approaches to targeted temperatures, and image capture
199   for fluorescence detection, this rapid thermocycling leads to completion of 50 cycles of PCR in less than
200   18 minutes.
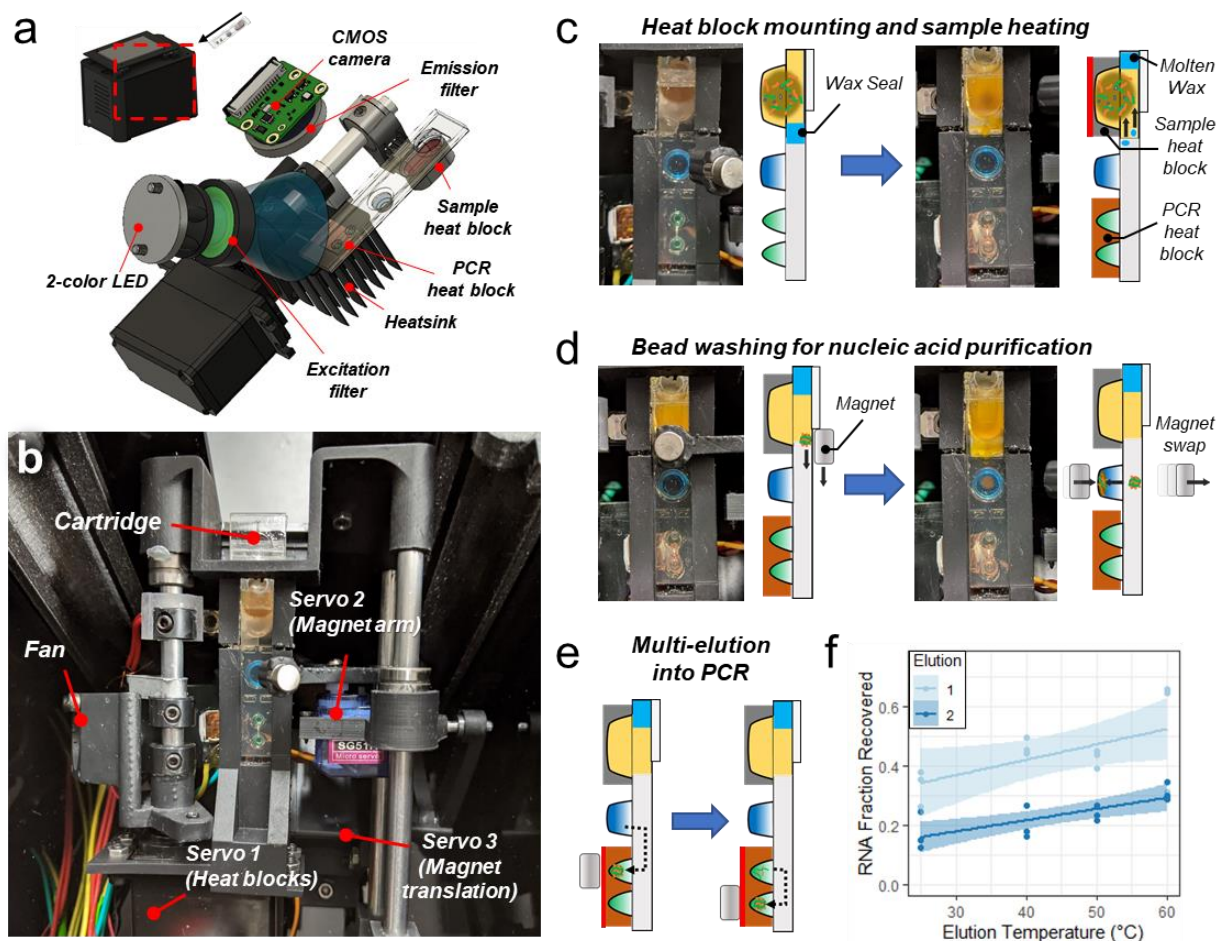
Fig. 3| Instrumentation for automated sample preparation and multi-elution. a, Fluorescence detection optics and heat blocks assembly. **b,** Servo motor arrangement for (1) mounting heat blocks onto the cartridge, (2) swiveling magnets to the top and bottom of the cartridge for bead extraction and introduction into wells, and (3) translating the magnet arm along the cartridge for bead transfer between wells. **c,** Rotation of the heat blocks mounts them onto the cartridge followed by sample well heating to promote sample lysis and melt the wax seal. **d,** Translation of the top magnet from the sample well to the wash well followed by swiveling the magnet arm to swap the bottom magnet into close proximity with the cartridge pulls the beads into the wash buffer. **e,** Sequential transfer of beads into the first PCR well and then the second elutes captured RNA into both reactions. **f,** The first elution releases more RNA than the second elution with tunable release of the overall fraction of RNA by changing temperature of the buffer during elution. Both elution steps were run in triplicate at each temperature condition and shown here fit with a linear regression with 95% confidence interval bands.

Assay cartridge analytical sensitivity and specificity

Throughout thermocycling, the CMOS camera takes a picture of the PCR wells for each fluorescence channel at the end of each cycle's annealing step (Fig. 4a). The pixel intensity for each well is isolated and averaged to generate a real-time fluorescence curve (Fig. 4b), from which the cycle threshold (Ct) is determined with an automated thresholding algorithm (Supplementary Fig. 6). Detection of amplification and Ct calculation is conducted at the end of each cycle during the test for live reporting of results to the user. For high viral load samples (Ct <20), detection of targets may be reported within 18 minutes from insertion of the cartridge into the instrument.

221   Using the respiratory panel cartridge design, 50 µL samples containing serial dilutions of
222   inactivated SARS-CoV-2, influenza A, or influenza B viral particles were loaded into cartridges with
223   magnetic bead solutions. Each dilution was run in triplicate. Both SARS-CoV-2 and Influenza A were
224   detectable in all replicates down to 2 copies/µL of sample (Figs. 4c-f), while Influenza B was detected down
225   to 24 copies/µL of sample (Figs. 4g, h). We also demonstrated detection of SARS-CoV-2 spiked into saliva
226   with a limit of detection of 12.5 copies/µL (Supplementary Fig. 7). To assess the specificity of the assay,
227   the cartridges were run using a panel of 14 viral and bacterial pathogens (Supplementary Table 2). No
228   cross-reactive false-positive amplification was detected for any pathogens in the specificity testing panel.
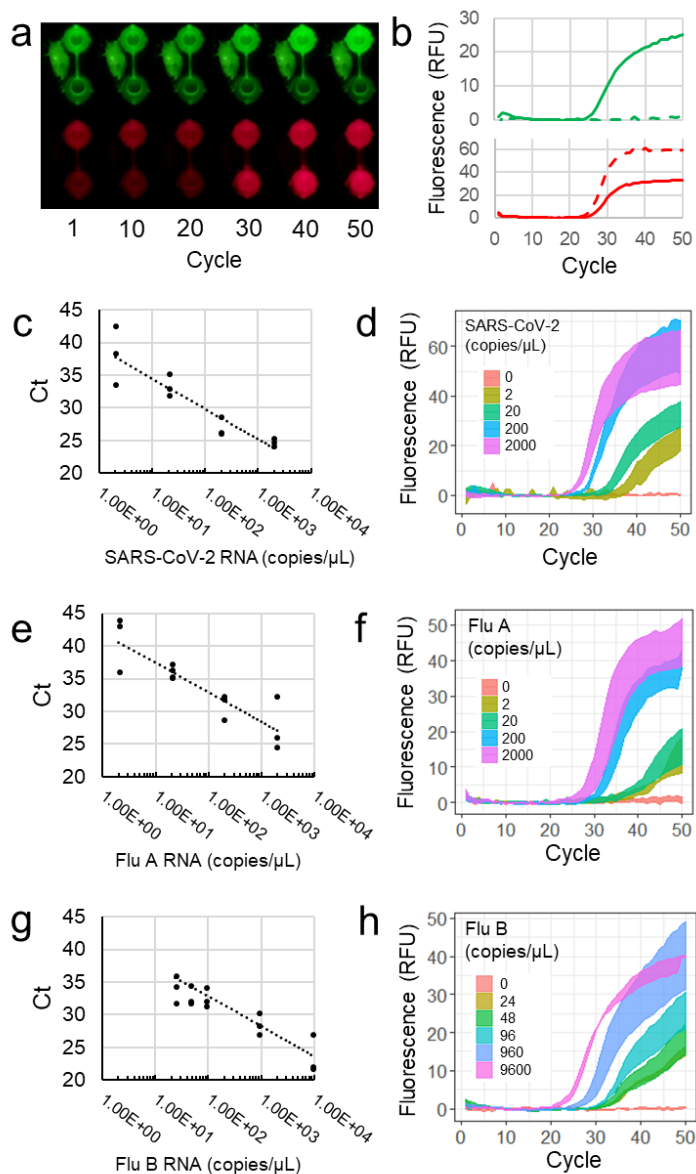
229

230   **Fig 4| Cartridge PCR fluorescence curves and analytical sensitivity. a,** Fluorescence images of PCR wells in the FAM
231   and Cy5 channels taken at the annealing step for each cycle with corresponding real-time fluorescence curves
232   plotted in (**b**). Solid lines and dotted lines in (**b**) correspond to the top and bottom wells respectively. Standard curves

233 with Ct values and corresponding average of triplicate fluorescence curves with standard error are shown for SARS-
234 CoV-2 (**c-d**), influenza A (**e-f**)**,** and influenza B (**g-h**).

235 *Clinical sample validation*

236 Using the cartridge for detection of SARS-CoV-2 variants we evaluated clinical samples from Johns
237 Hopkins Hospital (JHH) as well as extracted RNA from B.1.1.7 and B.1.351 variants. All samples were
238 previously classified by sequencing using the ARTIC protocol[31] into three categories as either (1) B.1.1.7,
239 (2) B.1.351/P.1, or (3) Other, indicating sample did not possess the characteristic mutations of current
240 variants of concern (Table 1). All JHH samples (*n* = 4) amplified N1, ORF1a, and spike targets indicating
241 they were not one of the variants of concern. Samples previously classified as B.1.1.7 variants (*n* = 4) by
242 sequencing produced fluorescent amplification signals for N1 on cartridge, but no amplification of either
243 the ORF1a or the spike targets and were accordingly classified properly. The samples characterized as
244 B.1.351 (*n* = 3) by sequencing produced signals for N1 and spike, but did not amplify the ORF1a target
245 resulting in proper classification as B.1.351 or P.1.

246 **Table 1. Detection of SARS-CoV-2 Variants**

| Sample	N1-Ct	ORF1a-Ct	Spike-Ct	Classification
JHH #1	30.39	32.57	32.64	Other
JHH #2	30.78	34.44	33.85	Other
JHH #3	28.73	38.10	27.49	Other
JHH #4	28.33	45.57	27.54	Other
B.1.1.7 #1	26.03	Not detected	Not detected	B.1.1.7
B.1.1.7 #2	32.03	Not detected	Not detected	B.1.1.7
B.1.1.7 #3	34.38	Not detected	Not detected	B.1.1.7
B.1.1.7 #4	30.13	Not detected	Not detected	B.1.1.7
B.1.351 #1	33.03	Not detected	37.59	B.1.351 or P.1
B.1.351 #2	28.29	Not detected	37.59	B.1.351 or P.1
B.1.351 #3	32.78	Not detected	31.49	B.1.351 or P.1

247

248 To assess performance of the respiratory pathogen panel cartridges, we tested clinical swab
249 eluates (*n* = 116) and passive drool saliva (*n* = 14). As a comparator assay, samples were first assessed with
250 a benchtop assay adapted from the CDC recommended protocol (Supplementary Fig. 8)[32]. Of the swab
251 samples, 54 were positive for SARS-CoV-2, 14 were Flu A positive, and 4 were Flu B positive using cutoff
252 Ct values at 45, 49, and 47 respectively. Saliva samples contained 7 SARS-CoV-2 positives all of which were
253 correctly classified with the cartridge assay. Only one of the SARS-CoV-2 samples went undetected in
254 cartridge, which was a swab eluate with a relatively late Ct (37.2) by the benchtop comparator assay
255 indicating a low viral titer. Of the negative SARS-CoV-2 swab samples, three false-positives were detected
256 using cartridges, all with late Cts (> 39) indicative of possible low-level contamination from handling other
257 positive samples. Sensitivity and specificity for detection of SARS-CoV-2 from swabs was 96.3% (95%
258 confidence interval: 90.7-100%) and 95.2% (88.7-100%), respectively.

259 The cartridge Flu A assay missed detection of 2 out of the 14 positives which both had the lowest
260 viral load of the Flu A samples (Ct >35), but yielded full concordance with negative samples, resulting in a
261 sensitivity and specificity of 85.7 (64.3-100%) and 100%, respectively. For Flu B, all 4 positives were
262 detected in cartridge with just one false-positive resulting in a specificity of 98.2% (95.5-100%). We have

263   excluded 5 negative samples and 4 SARS-CoV-2 positive samples that produced invalid cartridge results

264   with no amplification of the control or any other targets (Supplementary Table 3). These invalid results

265   may be a consequence of samples with relatively high levels of inhibitory compounds.

266
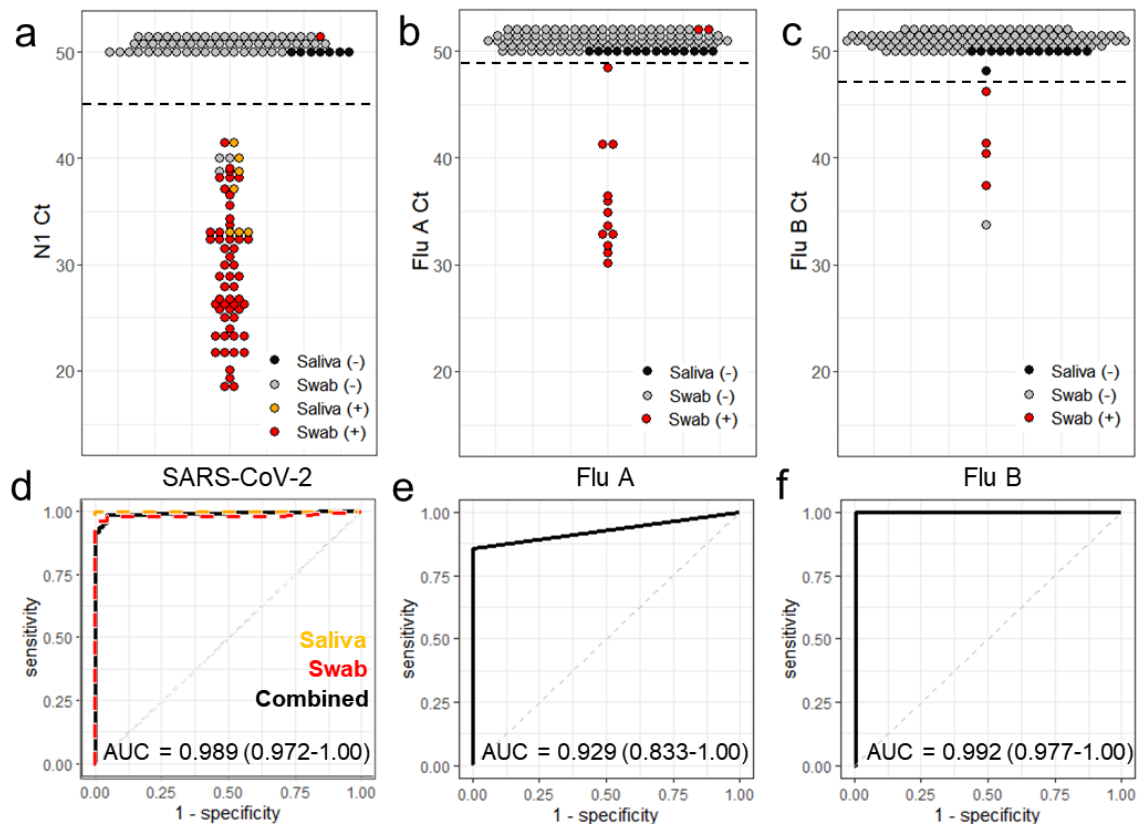
268   **Fig. 5| Clinical sample validation. a-c,** PCR cycle threshold (Ct) values for swabs (n = 116) and saliva samples (n = 14)
269   run in the multiplexed respiratory panel cartridges. Each point represents one sample with positive (+) and negative
270   (-) classification determined by the benchtop comparator assay and denoted by color. All reactions with
271   undetectable amplification are plotted with a Ct of 50 or higher. Cutoff Ct values for each assay are indicated with a
272   horizontal dashed line. **d-f,** Corresponding receiver operator curves for the SARS-CoV-2, Flu A, and Flu B cartridge
273   assays. Area under the curve (AUC) is indicated with 95% confidence interval.

274   **Discussion**

275   There is an urgent need for affordable and mass-produced testing options that can provide rapid,
276   multiplexed results for identification of variants and to allow future screening of SARS-CoV-2 with other
277   diseases that produce similar respiratory symptoms. Compared to the intricate multi-component designs
278   of current commercially available cartridges, our simple thermoplastic cartridges demonstrate great
279   potential as a highly cost-effective and scalable solution, which is amenable to industrial manufacturing
280   techniques such as roll-to-roll molding, lamination, and die-cutting.

281   Numerous *in vitro* diagnostic companies and researchers propose the use of isothermal NATs as PCR
282   alternatives to leverage the sensitivity of RNA-based detection while reducing cost with simplified
283   instrumentation or "instrumentation-free" testing[33,34]. These tests have been developed using isothermal

284 techniques such as loop-mediated isothermal amplification (LAMP)[35,36], recombinase polymerase
285 amplification (RPA)[37], or CRISPR-Cas based detection of viral RNA[38]. However, the need for manual
286 processes to purify and concentrate sample RNA to achieve high sensitivity assays is often overlooked.
287 Our magnetofluidic cartridges completely automate nucleic acid purification and concentration and
288 minimize user intervention for reading results.

289 Our platform enables detection of multiple SARS-CoV-2 variants or other respiratory pathogens, while
290 traditional rapid lateral-flow antigen tests and isothermal tests typically lack the ability to multiplex
291 detection of several pathogens without either setting up multiple separate tests or requiring further post-
292 processing steps for detection[39–41]. Post-processing of amplified products for readout of results adds an
293 additional manual step which reduces the likelihood of adoption where a high-volume of tests requires
294 minimal hands-on time. Furthermore, any handling of amplified product raises risks of contamination
295 which would compromise test specificity.

296 Most low-cost rapid tests have minimal connectivity, making streamlined acquisition of patient results
297 for surveillance difficult and can result in under-reporting of cases[42]. For widespread adoption, on-site
298 multiplexed diagnostic methods need a user workflow as simple, fast, and affordable as lateral flow strips
299 while maintaining connectivity for connecting to clinical databases for improving surveillance. This
300 platform meets these needs in a compact user-friendly format that is compatible with various sample
301 types including PBS, universal transport media, and saliva.

302 For realistic deployment, there are a few limitations to the current platform that must be addressed.
303 In particular, the current cartridges are not shelf-stable for prolonged storage at room-temperature and
304 are refrigerated or frozen prior to use. We are currently investigating techniques for built-in storage of
305 dry reagents to allow stability at ambient conditions. To include testing for additional variants or
306 respiratory pathogens, the cartridge would need to be expanded from the current 2-well design with
307 additional PCR wells for higher multiplexing. Given the limited clinical sample volume available in this
308 study, the assay design used a maximum 50 µL input per sample, though further improvement to
309 sensitivity to prevent false-negatives may be achieved by adapting the cartridge and binding buffer to be
310 compatible with larger volumes of sample.

311 **Methods**

312 *RT-PCR assay composition*

313 A 7.5-µL duplexed PCR probe assay was composed of 1X qScript XLT 1-Step RT-qPCR ToughMix
314 (QuantaBio), 0.1 U/µL SpeedSTAR HS DNA polymerase (Takara Bio), 0.1 U/µL AccuStart II Taq DNA
315 polymerase (QuantaBio), 1 mg/mL BSA (New England Biolabs), 0.1 % Tween-20 (Sigma Aldrich) and
316 primer-probe pairs. For duplexed assay for N1 and control RNA, the assay contains 1 µM each N1 primer,
317 0.45 µM each Luciferase primer, 1 µM N1 probe and 0.25 µM Luciferase probe. For duplexed assay for
318 influenza A and influenza B, the assay contains 0.5 µM each influenza A primer, 1 µM each influenza B
319 primer, 0.25 µM influenza A probe and 0.5 µM influenza B probe. For duplexed assay of SARS-CoV-2
320 variant detection, the assay contains 0.67 µM each Yale Spike Δ69-70 primer, 0.3 µM each Yale ORF1a
321 Δ3675-3677 primer, 0.2 µM Yale Spike Δ69-70 probe and 0.2 µM ORF1a Δ3675-3677 probe. All
322 oligonucleotides, including primers and fluorescently labeled DNA probe (sequences in Supplementary
323 Table 4) were purchased from Integrated DNA Technologies.

324   *Cartridge fabrication and assembly*

325   The magnetofluidic cartridges were assembled from three thermoplastic layers (Supplementary
326   Fig. 2). The bottom layer was fabricated by thermoforming 10 mil (~0.25 mm) thick polyethylene
327   terephthalate glycol (PETG) sheet (Welch Fluorocarbon) over 3D-printed molds (Form 2, Formlabs)
328   designed in Fusion 360 (Autodesk) to produce extruded wells. The middle layer was laser-cut from 0.75
329   mm thick acrylic (ePlastics) with pressure-sensitive adhesive (PSA) (9472LE adhesive transfer tape, 3M)
330   laminated on both sides. The top layer was laser-cut from 1.5 mm thick clear acrylic sheet (McMaster-
331   Carr, USA) with Teflon tape (McMaster-Carr) laminated to one side and patterned by laser-etching.

332   To load reagents into the cartridge wells, the thermoformed section and acrylic middle layer were
333   first joined with PSA, followed by dispensing 7.5 µL PCR solution and 50 µL wash buffer (W14,
334   ChargeSwitch Total RNA Cell Kit, Invitrogen) into corresponding wells. With aqueous reagents pre-loaded,
335   the cartridge was sealed by lamination with the top layer using the PSA on the other side of the middle
336   layer. Once sealed, 420 µL silicone oil (100 cSt, Millipore-Sigma) was injected through the sample injection
337   port to cover the wells and fill the remaining space within the cartridge except for the first well. To create
338   the wax plug in the first well, 40 µL of molten docosane wax (Millipore-Sigma) was dispensed into the
339   sample port and melted into the oil with a custom heating rig followed by cooling at room temperature
340   to solidify. The cartridge was either used immediately or the sample injection port was sealed with
341   adhesive tape (Scotch Magic Tape, 3M) and the cartridge stored on ice or frozen until use.

342   *Instrument design*

343   Laser-cut and 3D-printed housing and fixtures of the instrument was designed in Fusion 360.
344   External walls were laser-cut from 1/8" thick acrylic (McMaster-Carr) and 3D-printed components were
345   fabricated using an SLA (Form 2, Black Resin, Formlabs) or FDM printer (Prusa Mini, Prusament PETG,
346   Prusa research). A 5-inch HDMI touchscreen (Elecrow) was mounted on top of the instrument to allow
347   user input with the graphic user interface (GUI) designed in python using the Tkinter library. Motorized
348   actuation of an arm containing opposing neodymium magnets (K&J Magnetics) was implemented with a
349   micro servo motor (TowerPro SG51R) mounted on a carriage guided along two aluminum rails by a second
350   servo motor (Hitec HS-485HB). A third servo motor (Hitec HS-485HB) pivoted an aluminum rod to swivel
351   the heat blocks onto the cartridge. The sample well heat block was custom machined out of 6061
352   aluminum and mounted onto a power resistor (Riedon PF1262-5RF1) with a steel M3 screw, while the
353   PCR heat block was machined from 145 copper and mounted onto a thermoelectric element (Peltier Mini
354   Module, Custom Thermoelectric) and heatsink using thermally conductive epoxy (Arctic Alumina Thermal
355   Adhesive, Arctic Silver). Temperature of the heat blocks was monitored with a thermistor probe
356   (GA100K6MCD1, TE Connectivity) epoxied directly adjacent to the wells. A 5V fan (Sunon) provided
357   cooling to the heatsink.

358   Cartridges were illuminated using the red and blue channels of a 3-color RGB LED (Vollong) passed
359   through a focusing lens (10356, Carclo) and dual bandpass excitation filter (59003m, Chroma).
360   Fluorescence was captured with a CMOS camera (Pi NoIR Camera V2, Raspberry Pi) through a dual
361   bandpass emission filter (535-700DBEM, Omega Optical). An Arduino Nano microcontroller coordinated
362   control of the LEDs, fan, and motors, and a Raspberry Pi 3B+ ran the GUI, processed fluorescence images,
363   monitored thermistor readings and provided current to the heat blocks via a motorshield (Dual
364   TB9051FTG Motor Driver, Pololu). Power to the instrument was supplied with a 7.5V 45W wall adapter
365   (MEAN WELL GST60A07-P1J).

Cartridge limit of detection determination

Limit of detection of the cartridge assays was determined using contrived specimens of viral particles spiked into nasopharyngeal swab or saliva samples. Gamma-irradiated viral particles from SARS-Related Coronavirus 2 (Isolate USA-WA1/2020), Influenza A/Puerto Rico/8/1934-9VMC2(NR-29027), and Influenza B virus B/Nevada/03/2011 (BV) (NR-44023) were obtained through the BEI Resources Repository and stored at -80 °C upon receipt. To prepare the contrived samples, a serial dilution of viral particles were spiked into pooled (*n* = 4) clinical specimens (confirmed PCR-negative by the Johns Hopkins Clinical Microbiology Lab). Each concentration was tested a minimum of three times, and the limit of detection was determined when one of the replicates showed negative. Fifty microliters of swab eluate or five microliters of saliva was first mixed with 150 µL magnetic bead binding buffer consisting of 0.67 mg/mL ChargeSwitch beads, 0.5M KCl in 100mM aqueous MES, and 10^5 copies of Luciferase RNA internal control (Promega). The entire mixture of sample and bead buffer was loaded into the sample port of the cartridge followed by insertion into the instrument for processing.

Clinical sample testing

Clinical swab and saliva specimens were previously collected under Johns Hopkins IRB #00246027. Specimens were de-identified and blinded before testing. Nasopharyngeal swabs were eluted in 3 mL of Universal Transport Medium. Passive drooled saliva specimens were collected into an empty vessel. Five microliters of saliva was lysed with 50 µL of aqueous buffer containing 1% Triton X-100 and 1.2 units of Thermolabile Proteinase K (P8111S, New England Biolabs). 50 µL of swab eluate or 55 µL of saliva with lysis buffer was mixed with 150 µL magnetic bead binding buffer as previously described followed by loading the entire mixture into the sample port of the cartridge. The comparator assay for evaluation of clinical samples used a modified CDC testing protocol[32] for swabs (Supplementary Methods, Supplementary Fig. 8) and FDA EUA authorized SalivaDirect protocol[43] for saliva were employed to test all the clinical specimens on a Bio-Rad CFX96 Touch Real-Time PCR System as reference.

Testing of SARS-CoV-2 variants used RNA from clinical samples extracted using a chemagic 360 instrument (PerkinElmer) with clades of each sample previously characterized by sequencing[31]. 2 µL of extracted RNA was mixed with 150 µL magnetic bead binding buffer following by loading into the sample port of the cartridge.

Acknowledgements

Competing Interests

AYT and T-HW are coinventors on patent PCT/US2019/029937 "A Disposable Reagent Scaffold for Biochemical Process Integration".

Supplementary Materials

Supplementary Methods

Supplementary Figures List

Fig. S1. Loading Cartridges and Instrument Operation

Fig. S2. Cartridge Assembly

Fig. S3. Nucleic Acid Aliquoting with Sequential Elution

Fig. S4. Servo actuation for cartridge mounting and magnetic transfer

Fig. S5. Heat block simulation and design for rapid thermocycling

Fig. S6. Fluorescence processing algorithm

Fig. S7. Detection of SARS-CoV-2 in saliva

Fig. S8. Comparator assay evaluation

Supplementary Tables List

Table 1. Instrument bill of materials

Table 2. Specificity testing

Table 3. Clinical samples data

Table 4. PCR primers and probes

Supplementary Movies

Movie S1. On-cartridge sample processing

References

1.   Sutton, D., Fuchs, K., D'Alton, M. & Goffman, D. Universal Screening for SARS-CoV-2 in Women Admitted for Delivery. *N. Engl. J. Med.* **382**, 2163–2164 (2020).

2.   Kucharski, A. J. *et al.* Effectiveness of isolation, testing, contact tracing, and physical distancing on reducing transmission of SARS-CoV-2 in different settings: a mathematical modelling study. *Lancet Infect. Dis.* **20**, 1151–1160 (2020).

3.   Peto, J. *et al.* Weekly COVID-19 testing with household quarantine and contact tracing is feasible and would probably end the epidemic: Weekly Covid-19 testing. *R. Soc. Open Sci.* **7**, 0–3 (2020).

4.   Galloway, S. E. *et al.* Emergence of SARS-CoV-2 B.1.1.7 Lineage — United States, December 29, 2020–January 12, 2021. *MMWR. Morb. Mortal. Wkly. Rep.* **70**, 95–99 (2021).

5.   Volz, E. *et al.* Transmission of SARS-CoV-2 Lineage B.1.1.7 in England: Insights from linking epidemiological and genetic data. *medRxiv* 2020.12.30.20249034 (2021).

435   6.   Lauring, A. S. & Hodcroft, E. B. Genetic Variants of SARS-CoV-2 - What Do They Mean? *JAMA - J.*
436   *Am. Med. Assoc.* **325**, 529–531 (2021).

437   7.   Grubaugh, N. D., Hodcroft, E. B., Fauver, J. R., Phelan, A. L. & Cevik, M. Public health actions to
438   control new SARS-CoV-2 variants. *Cell* **184**, 1127–1132 (2021).

439   8.   Veldhoen, M. & Simas, J. P. Endemic SARS-CoV-2 will maintain post-pandemic immunity. *Nat.*
440   *Rev. Immunol.* (2021). doi:10.1038/s41577-020-00493-9

441   9.   Gwinn, M., MacCannell, D. & Armstrong, G. L. Next-Generation Sequencing of Infectious
442   Pathogens. *JAMA* **321**, 893 (2019).

443   10.   Vogels, C. B. *et al.* PCR assay to enhance global surveillance for SARS-CoV-2 variants of concern.
444   *medRxiv* **351**, 2021.01.28.21250486 (2021).

445   11.   Babiker, A., Myers, C. W., Hill, C. E. & Guarner, J. SARS-CoV-2 Testing. *Am. J. Clin. Pathol.* **153**,
446   706–708 (2020).

447   12.   WHO. Laboratory testing for 2019 novel coronavirus (2019-nCoV) in suspected human cases.
448   Interim guidance. (2020). Available at: https://www.who.int/publications/i/item/10665-331501.
449   (Accessed: 6th December 2020)

450   13.   McGarry, B. E., SteelFisher, G. K., Grabowski, D. C. & Barnett, M. L. COVID-19 Test Result
451   Turnaround Time for Residents and Staff in US Nursing Homes. *JAMA Intern. Med.* **181**, 556
452   (2021).

453   14.   Peeling, R. W. *et al.* Serology testing in the COVID-19 pandemic response. *Lancet Infect. Dis.* **20**,
454   e245–e249 (2020).

455   15.   Foundation for Innovative New Diagnostics (FIND). FIND evaluation update: SARS-CoV-2 Assays.
456   Available at: https://www.finddx.org/covid-19/sarscov2-eval/. (Accessed: 6th December 2020)

457   16.   Weissleder, R., Lee, H., Ko, J. & Pittet, M. J. COVID-19 diagnostics in context. *Sci. Transl. Med.* **12**,
458   1–7 (2020).

459   17.   Pipper, J. *et al.* Catching bird flu in a droplet. *Nat. Med.* **13**, 1259–1263 (2007).

460   18.   Shin, D. J. & Wang, T. H. Magnetic Droplet Manipulation Platforms for Nucleic Acid Detection at
461   the Point of Care. *Ann. Biomed. Eng.* **42**, 2289–2302 (2014).

462   19.   Zhang, Y. & Nguyen, N.-T. Magnetic digital microfluidics – a review. *Lab Chip* **17**, 994–1008
463   (2017).

464   20.   Egatz-Gómez, A. *et al.* Discrete magnetic microfluidics. *Appl. Phys. Lett.* **89**, (2006).

465   21.   Shin, D. J. *et al.* Mobile nucleic acid amplification testing (mobiNAAT) for Chlamydia trachomatis
466   screening in hospital emergency department settings. *Sci. Rep.* **7**, 4495 (2017).

467   22.   Shin, D. J., Trick, A. Y., Hsieh, Y. H., Thomas, D. L. & Wang, T. H. Sample-to-Answer Droplet
468   Magnetofluidic Platform for Point-of-Care Hepatitis C Viral Load Quantitation. *Sci. Rep.* **8**, (2018).

469   23.   Trick, A. Y. *et al.* A portable magnetofluidic platform for detecting sexually transmitted infections
470   and antimicrobial susceptibility. *Sci. Transl. Med.* **13**, (2021).

471   24.   Goldenberger, D. *et al.* Brief validation of the novel GeneXpert Xpress SARS-CoV-2 PCR assay. *J.*

472   *Virol. Methods* **284**, 113925 (2020).

473   25.   Liotti, F. M. *et al.* Evaluating the newly developed BioFire COVID-19 test for SARS-CoV-2
474   molecular detection. *Clin. Microbiol. Infect.* **26**, 1699–1700 (2020).

475   26.   Johnson, D. R., Lee, P. K. H., Holmes, V. F. & Alvarez-Cohen, L. An internal reference technique for
476   accurately quantifying specific mRNAs by real-time PCR with application to the tceA reductive
477   dehalogenase gene. *Appl. Environ. Microbiol.* **71**, 3866–3871 (2005).

478   27.   Lu, X. *et al.* US CDC Real-Time Reverse Transcription PCR Panel for Detection of Severe Acute
479   Respiratory Syndrome Coronavirus 2. *Emerg. Infect. Dis.* **26**, 1654–1665 (2020).

480   28.   Van Elden, L. J. R., Nijhuis, M., Schipper, P., Schuurman, R. & Van Loon, A. M. Simultaneous
481   detection of influenza viruses A and B using real-time quantitative PCR. *J. Clin. Microbiol.* **39**,
482   196–200 (2001).

483   29.   Terrier, O. *et al.* Cellular transcriptional profiling in human lung epithelial cells infected by
484   different subtypes of influenza A viruses reveals an overall down-regulation of the host p53
485   pathway. *Virol. J.* **8**, 285 (2011).

486   30.   World Health Organization. WHO information for the molecular detection of influenza viruses.
487   (2020). Available at:
488   https://www.who.int/influenza/gisrs_laboratory/Protocols_influenza_virus_detection_Jan_2020.
489   pdf. (Accessed: 27th February 2021)

490   31.   Thielen, P. M. *et al.* Genomic diversity of SARS-CoV-2 during early introduction into the
491   Baltimore-Washington metropolitan area. *JCI Insight* **6**, (2021).

492   32.   Centers for Disease Control and Prevention (CDC). CDC 2019-Novel Coronavirus (2019-nCoV)
493   Real-Time RT-PCR Diagnostic Panel, Revision: 06. (2020).

494   33.   Peto, J., Hunter, D. J., Riboli, E. & Griffin, J. L. Unnecessary obstacles to COVID-19 mass testing.
495   *Lancet* **396**, 1633 (2020).

496   34.   Woo, C. H., Jang, S., Shin, G., Jung, G. Y. & Lee, J. W. Sensitive fluorescence detection of SARS-
497   CoV-2 RNA in clinical samples via one-pot isothermal ligation and transcription. *Nat. Biomed. Eng.*
498   **4**, 1168–1179 (2020).

499   35.   Dao Thi, V. L. *et al.* A colorimetric RT-LAMP assay and LAMP-sequencing for detecting SARS-CoV-2
500   RNA in clinical samples. *Sci. Transl. Med.* **12**, (2020).

501   36.   Ganguli, A. *et al.* Rapid isothermal amplification and portable detection system for SARS-CoV-2.
502   *Proc. Natl. Acad. Sci.* **117**, 22727–22735 (2020).

503   37.   Behrmann, O. *et al.* Rapid Detection of SARS-CoV-2 by Low Volume Real-Time Single Tube
504   Reverse Transcription Recombinase Polymerase Amplification Using an Exo Probe with an
505   Internally Linked Quencher (Exo-IQ). *Clin. Chem.* **66**, 1047–1054 (2020).

506   38.   Broughton, J. P. *et al.* CRISPR–Cas12-based detection of SARS-CoV-2. *Nat. Biotechnol.* **38**, 870–
507   874 (2020).

508   39.   Gootenberg, J. S. *et al.* Multiplexed and portable nucleic acid detection platform with Cas13,
509   Cas12a and Csm6. *Science (80-.).* **360**, 439–444 (2018).

510   40.   Xu, G. *et al.* Paper-Origami-Based Multiplexed Malaria Diagnostics from Whole Blood. *Angew.*
511   *Chemie* **128**, 15476–15479 (2016).

512   41.   Daher, R. K., Stewart, G., Boissinot, M. & Bergeron, M. G. Recombinase polymerase amplification
513   for diagnostic applications. *Clin. Chem.* **62**, 947–958 (2016).

514   42.   Pradhan, R., Weber, L. & Recht, H. Lack of Antigen Test Reporting Leaves Country 'Blind to the
515   Pandemic'. *Kaiser Health News* (2020). Available at: https://khn.org/news/lack-of-antigen-test-
516   reporting-leaves-country-blind-to-the-pandemic/. (Accessed: 21st April 2021)

517   43.   FDA. Yale School of Public Health, Department of Epidemiology of Microbial Diseases SalivaDirect
518   assay EUA Summary – Updated April 9, 2021. Available at:
519   https://www.fda.gov/media/141192/download. (Accessed: 21st April 2021)